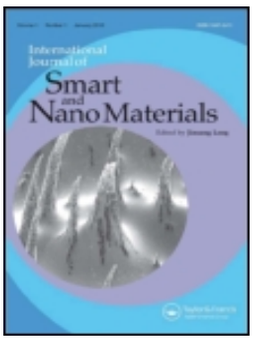

International Journal of Smart and Nano Materials

ISSN: 1947-5411 (Print) 1947-542X (Online) Journal homepage: http://www.tandfonline.com/loi/tsnm20

Epoxy resin nanocomposites reinforced with ionized liquid stabilized carbon nanotubes

Zhe Wang , Xiongtao Yang , Qiang Wang , H. Thomas Hahn , Sang-gi Lee , Kun-Hong Lee & Zhanhu Guo

To cite this article: Zhe Wang , Xiongtao Yang , Qiang Wang , H. Thomas Hahn , Sang-gi Lee , Kun-Hong Lee & Zhanhu Guo (2011) Epoxy resin nanocomposites reinforced with ionized liquid stabilized carbon nanotubes, International Journal of Smart and Nano Materials, 2:3, 176-193, DOI: 10.1080/19475411.2011.594104

To link to this article: http://dx.doi.org/10.1080/19475411.2011.594104

International Journal of Smart and Nano Materials
Vol. 2, No. 3, September 2011, 176–193

Taylor & Francis
Taylor & Francis Group

Epoxy resin nanocomposites reinforced with ionized liquid stabilized carbon nanotubes

Zhe Wang[a], Xiongtao Yang[b], Qiang Wang[c], H. Thomas Hahn[a], Sang-gi Lee[d], Kun-Hong Lee[e] and Zhanhu Guo[b]*

[a]*Mechanical & Aerospace Engineering Department, University of California Los Angeles, Los Angeles, CA 90095, USA;* [b]*Integrated Composites Lab, Dan F. Smith Department of Chemical Engineering, Lamar University, Beaumont, TX 77710, USA;* [c]*Institute of Chemical and Engineering Sciences (ICES), A-STAR, Applied Catalysis, 1, Pesek Road, Jurong Island, 627833 Singapore;* [d]*Department of Chemistry and Nano Science, Ewha Womans University, Seoul 120-750, Korea;* [e]*Department of Chemical Engineering, Pohang University of Science and Technology, Pohang 790-784, Korea*

(*Received 11 April 2011; final version received 1 June 2011*)

Epoxy resin nanocomposites reinforced with three different ionic liquid functionalized carbon nanotubes (f-CNTs) were fabricated by an *in situ* polymerization method. The influence of the anions on the curing process was studied through differential scanning calorimetry (DSC) and normalized Fourier transform infrared (FTIR) spectroscopy. The composition of the nanocomposites was analyzed by X-ray photoelectron spectroscopy. Two different mechanisms are proposed to explain the curing process of the neat epoxy and its composites. The electric conductivity and mechanical properties of the nanocomposites are also reported. The tensile strength was increased dramatically due to the insertion of f-CNTs. Scanning electron microsopy fracture surface analysis indicates a strong interfacial bonding between the carbon nanotubes and the polymer matrix.

Keywords: epoxy resin; nanocomposite; carbon nanotube; ionic liquid functionalization

1. Introduction

Carbon nanotubes (CNTs) with high structural aspect ratio, excellent mechanical properties and superior electrical conductivity have led to interest in mass production techniques [1–4]. With CNTs having become commercially available in recent years, more effort from both academic and industrial communities has been put toward their applications. In fact, the CNTs have realized their first real application in terms of the CNTs-based nanostructural and functional materials [5–7]. CNT/polymer nanocomposites have been pursued with the aim of delivering the properties of the CNTs to the hosting polymer matrix [8–10]. Many polymers have been applied in the CNTs/polymer nanocomposites for various target applications. The introduction of the CNTs into a polymer matrix has improved the electrical conductivity as well as the mechanical properties of the polymer matrix [11–18].

*Corresponding author. Email: zhanhu.guo@lamar.edu

ISSN 1947-5411 print/ISSN 1947-542X online

DOI: 10.1080/19475411.2011.594104
http://www.informaworld.com

Ionic liquids (ILs), consisting of imidazolium cations and counter anions, have attracted increasing interest as fascinating materials for a wide range of synthesis, catalysis, electrochemistry and liquid–liquid extractions, due to their remarkable properties such as non-volatility, non-flammability, high ion density and extremely high ionic conductivity [19–23]. Some kinds of the polymer gel electrolytes containing ILs have been investigated with the aim of realizing both high ionic conductivity and good mechanical properties [24]. Polymer-in-IL electrolytes have also been prepared by *in situ* polymerization of vinyl monomers in ILs [25,26]. Ohno's group [27,28] has prepared the IL-type polymer films having flexible spacers between the polymerizable groups and the imidazolium cations. Polymerization of ILs is very effective to not only transport target ions but also improve mechanical properties. Although the polymeric ILs are flexible materials, their low mechanical strength limits their industrial applications.

In this work, epoxy resin nanocomposites were synthesized by *in situ* polymerization of the epoxy resin in the presence of three types of different ionized liquid functionalized CNTs (IL-CNTs) with different anions. The thermal properties of the epoxy resin nanocomposites reinforced with different IL-CNTs were measured by differential scanning calorimetry (DSC). X-ray photoelectron spectroscopy (XPS) was used to examine the interfacial interactions in the IL-CNTs/epoxy resin nanocomposites. The mechanical properties and the electrical conductivity of the nanocomposites were also investigated. The fracture surface of the nanocomposites was examined by scanning electron microscopy (SEM).

2. Experimental

2.1. Materials

The epoxy resin Epon 862 (bisphenol F epoxy) and EpiCure curing agent W were purchased from Miller-Stephenson Chemical Company, Inc. Other chemicals were purchased from Sigma-Aldrich Company. All the chemicals were used as-received without any further treatment.

2.2. Preparation of the IL-CNT/epoxy nanocomposites

The pristine epoxy resin was prepared by mixing EPON 862 with EpiCure curing agent W under mechanical stirring for 30 min, degassing the mixture in a vacuum oven at 80°C for 30 min. The ratio of Epon 862 and EpiCure W was 100:26. After the bubbles were completely removed, the mixture was transferred to stainless steel dog-bone molds and the complete curing was done for 4 h at 120°C. The cured material was then trimmed. Finally, the samples were machined for thermal and mechanical characterization.

Three different ionic liquid functionalized CNTs (PF_6-CNT, Cl-CNT, Br-CNT) were prepared, and Figure 1 shows their chemical structures [29,30]. The degree of functionalization was 1.3 mmol/g. Since the preparation process followed an acid-treatment process, the functional sites were located on the defects and ends of the CNTs. For the preparation of the PF_6-CNT and Cl-CNT epoxy nanocomposites, f-CNTs and the curing agent were sonicated in an ultrasonic bath for 4 h at room temperature and an additional 3 h at 70°C. Epon 862 was added and the three components were further shear mixed at 80°C for 30 min, and then sonicated for 30 min. The final mixture was degassed in a vacuum oven at 80°C for 2 h. The curing cycle of the epoxy nanocomposites was the same as that used for curing the neat epoxy. Since the ultrasonication was carried out for a short time at low-power in our experiments, no significant difference was observed in the properties of neat

cured epoxy which was prepared by following the composites preparation process and the regular curing process. The thickness of the final specimens was about 1.2 mm. Figure 2 shows the reaction scheme for the PF_6-CNT and Cl-CNT epoxy nanocomposites.

Due to the different surface functional groups attached on the CNT, Br-CNTs were first mixed with the preheated Epon to create the covalent bonding between the f-CNTs and the epoxy matrix. Subsequently, EpiCure curing agent W was added and further shear mixed with the Br-CNTs/Epon 862 mixture for 30 min and sonicated for 30 min. Finally, the resulting mixture was degassed in a vacuum oven at 80°C for 30 min. Then the curing cycle of the Br-CNTs/epoxy nanocomposites was the same as that of the pristine epoxy. Figure 3 illustrates the preparation procedure for the Br-CNT/epoxy nanocomposites.

2.3. Characterization

Tensile testing was performed using a micron tensile machine (Instron 4411) at room temperature in accordance with ASTM D 1708–06 a. The crosshead speed was 1 mm/s.

A scanning electron microscope (JEOL SM-71010) was used to examine the fracture surfaces. Fourier transform infrared (FTIR) spectra were recorded with a JASCO FTIR spectrometer analyzer, which was operated from 700 to 4000 cm^{-1} at room temperature. XPS spectra were recorded with a PHI-5702 Multi-Technique System ESCA/AES with a Mg Kα (1253.6 eV) source. The pressure in the analytical chamber was about 5×10^{-8} mbar. The correction of the electrostatic charging was made by adjusting the C1*s* signal of the aliphatic carbon atoms to 284.8 eV. Electric conductivity measurements were carried out using the two-point probe method.

The curing process was investigated by differential scanning calorimetry (DSC, Perkin Elmer Instruments) under 10 ccpm nitrogen flow conditions. The testing temperature was from 25 to 300°C with a heating rate of 5°C/min. The reaction enthalpy (J/g) and residual heat of reaction were measured from the area under the DSC peaks.

3. Results and discussion

3.1. DSC measurements of the curing process

The glass transition temperatures of the nanocomposites are determined on the basis of the DSC results. Figure 4 shows the DSC curves of the nanocomposites with 1 wt% f-CNT loading and pure epoxy. The glass transition temperatures of the polymer matrix depend on the free volume of the polymer, which is correlated to the affinity between the fillers and the polymer matrix [31,32]. Molecular motion in the bulk state depends on the presence of the vacancies or voids. The endothermic peak located at 120°C in each curve represents the glass transition temperature range for the corresponding nanocomposites. This indicates that the nanotubes prevent the epoxy from releasing energy at this temperature. Compared to cured neat epoxy samples, f-CNT/epoxy nanocomposites show a shoulder peak at around 150°C. The aforementioned reaction mechanism analysis indicates that the f-CNTs are inserted into the polymer matrix and there is a strong interaction between these two phases, which causes the change of crystallization behavior of the epoxy. Hence, the melting transition is also changed.

The total area under the heat flow peak, based on the extrapolated baseline at the end of the transition, was used to calculate the total heat of transition. The glass transition temperature and the heat of the transition (the transition enthalpy, ΔH) for each type of composites are reported in Table 1. It is obvious that the glass transition temperature

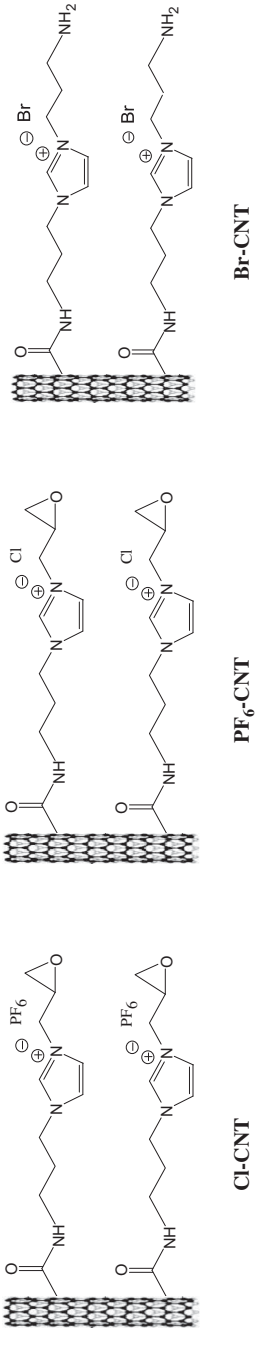

Figure 1. Structures of the ionized liquid functionalized CNTs.

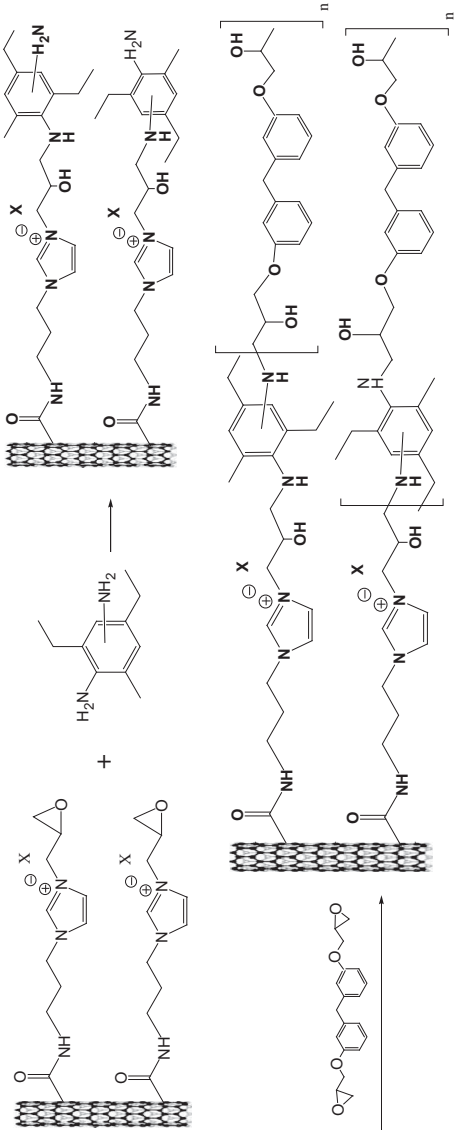

Figure 2. Chemical reactions for the synthesis of PF_6-CNT and Cl-CNT/epoxy resin nanocomposites.

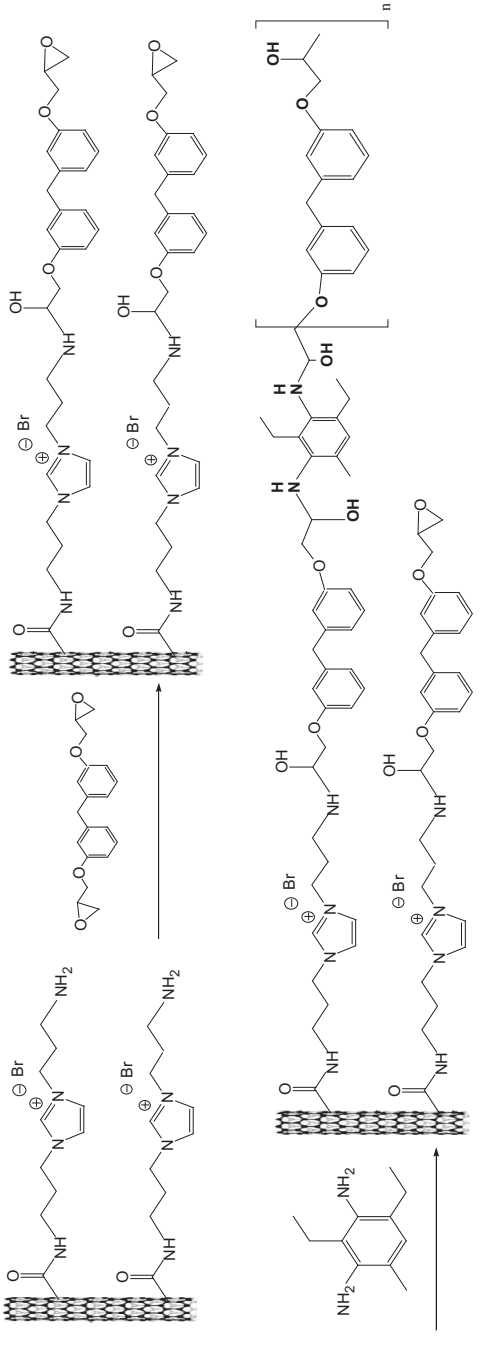

Figure 3. Chemical reactions for the synthesis of Br-CNT/epoxy resin nanocomposites.

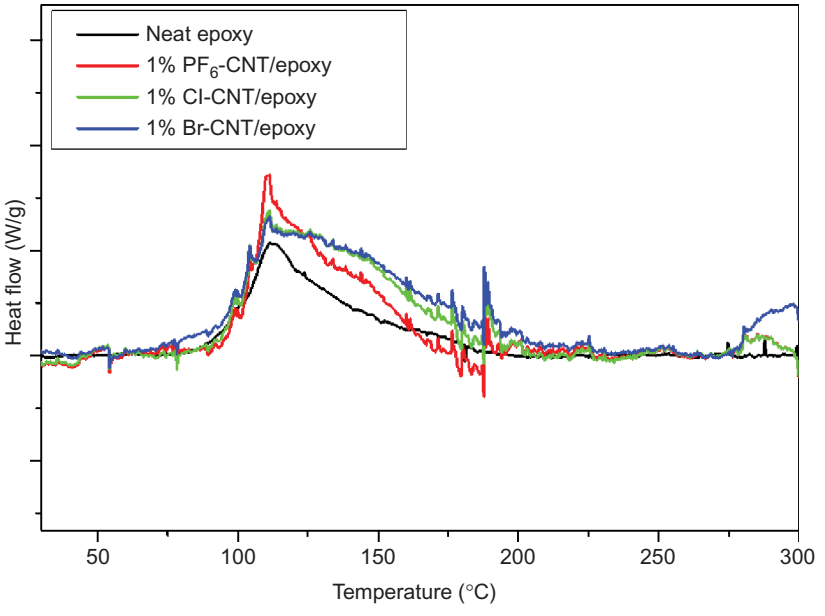

Figure 4. Dynamic DSC thermograms for the curing of neat epoxy and its nanocomposites.

Table 1. Peak temperature and endothermic enthalpy of the DSC cured samples.

Sample (1.0%)	T_g (°C)	ΔH (J/g)
Neat epoxy	112.5	16.04
PF_6-CNT/epoxy composite	113.8	21.27
Cl-CNT/epoxy composite	114.5	27.10
Br-CNT/epoxy composite	114.3	32.16

and ΔH decrease in the order of Br-CNT/epoxy, Cl-CNT/epoxy and PF_6-CNT/epoxy nanocomposites. Compared to the pure epoxy, the incorporation of the f-CNTs leads to an increase of the glass transition temperature in the f-CNT/epoxy resin nanocomposites. The covalent bonding between the f-CNT and the epoxy matrix is strong, which decreases the free volume of the nanocomposites and thus the glass transition temperature increases. Meanwhile, the ΔH value of the PF_6-CNT/epoxy nanocomposites is higher than that of the pure epoxy, whereas the ΔH values of the Cl-CNT/epoxy and Br-CNT/epoxy nanocomposites are slightly and significantly higher, respectively, than that of the pure epoxy. It is inferred that during the glass transition process, f-CNTs act as heat-shielding fillers and prevent the epoxy from exchanging energy with the outside system [33].

3.2. Curing kinetics

The DSC curing curves of neat epoxy and its Cl-CNT nanocomposites with different nanotube loadings are displayed in Figure 5. Only the main peak of the etherification reaction is observed and the reaction heat of the etherification reaction peak is approximately the total heat of the curing reaction. In addition, the functional groups on the chemically modified CNT surface act as the segments of the reaction agents to bridge the CNT and the

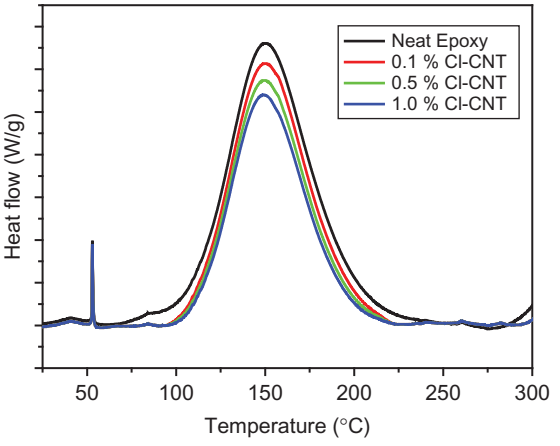

Figure 5. Dynamic DSC thermograms for the curing of the neat epoxy and its Cl-CNT/epoxy nanocomposites.

epoxy resin [31]. However, the released heat is much smaller than that of the curing reaction, which indicates that it can be considered to be negligible. Consequently, ΔH can be regarded as a constant over the whole curing reaction.

From a dynamic DSC run, the total area of the exothermal peak (the region between the exotherm and the baseline) is in direct proportion to the molar reaction heat, the ΔH released during the whole cure reaction [34,35]. The extent of the curing at any temperature can be expressed as

$$\alpha = \frac{\Delta H_s}{\Delta H} = \frac{A_s}{A}, \tag{1}$$

where ΔH_s is the heat of reaction of the partially cured samples heated up to the temperature T. The cure rate, $d\alpha/dt$, is defined by

$$\frac{d\alpha}{dt} = \frac{1}{\Delta H_0}\left(\frac{d\Delta H}{dt}\right)_T, \tag{2}$$

where α is the degree of curing, $(d\Delta H/dt)_T$ is the heat absorption rate during the scanning (J/s g = W/g) and ΔH_0 is the total amount of heat absorbed (J/g). Figures 6a–6c reveal a comparison of the curing kinetics at a heating rate of 5 K/min among the three types of f-CNT/epoxy nanocomposite systems;the value of α is included in Table 2.

3.3. Degree of curing by FTIR

The FTIR spectra of the neat epoxy resin and its Cl-CNT nanocomposites are presented in Figure 7. It is known that curing can be monitored by the FTIR technique [34,36]. In this study, the degree of curing of the f-CNT/epoxy nanocomposite was calculated. It is known that the epoxy group has three characteristic peaks in the fingerprint region: 830, 1250 and 913 cm^{-1} [31]. The band at 830 cm^{-1} is overlapped by the bending vibration of the two adjacent hydrogen atoms in the benzene ring. However, the feature at 913 cm^{-1} exhibits no interference [33,37]. The intensity of the band at 913 cm^{-1} decreases with increasing

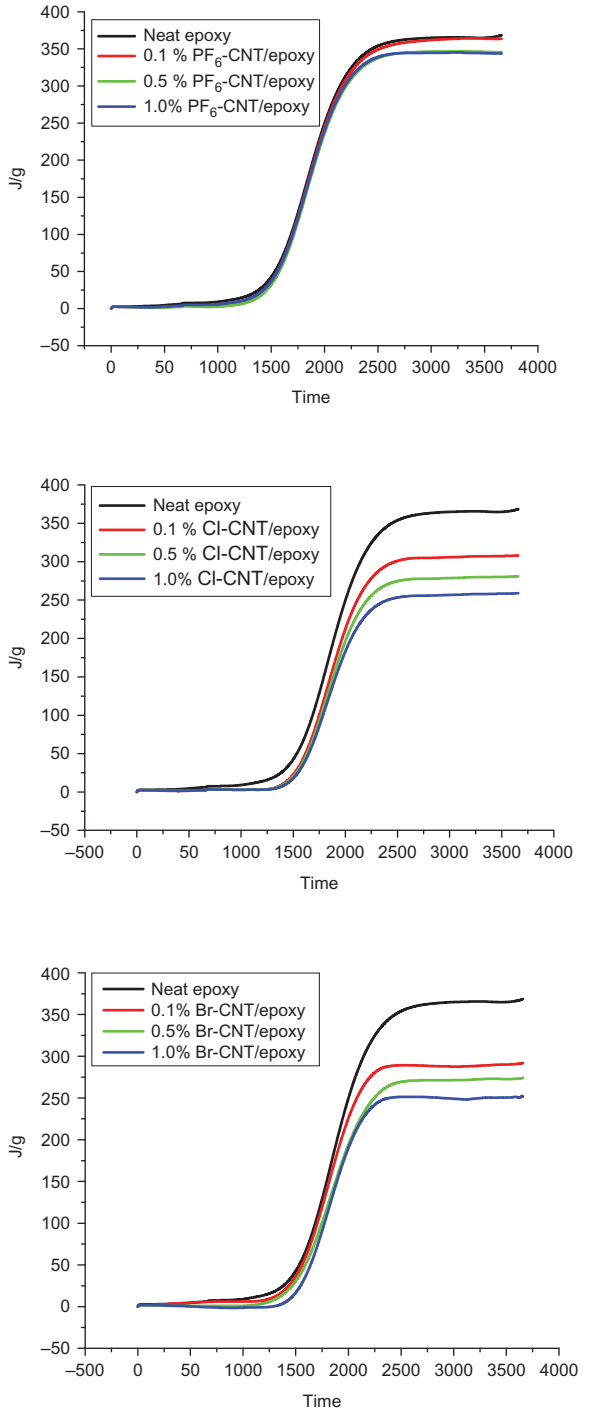

Figure 6. Advancement of the curing for the non-isothermal curing at 5 K/min heating rate of three types of composite samples. Lines are given only for showing the tendency.

Table 2. Degree of curing calculated by DSC and FTIR.

	PF_6-CNT		Cl-CNT		Br-CNT	
Loading	DSC	FTIR	DSC	FTIR	DSC	FTIR
0.10%	98.7%	98.2%	83.6%	84.3%	79.2%	81.2%
0.50%	93.8%	94.9%	76.2%	75.1%	74.3%	75.3%
1.00%	93.3%	94.5%	70.3%	73.6%	68.2%	70.2%

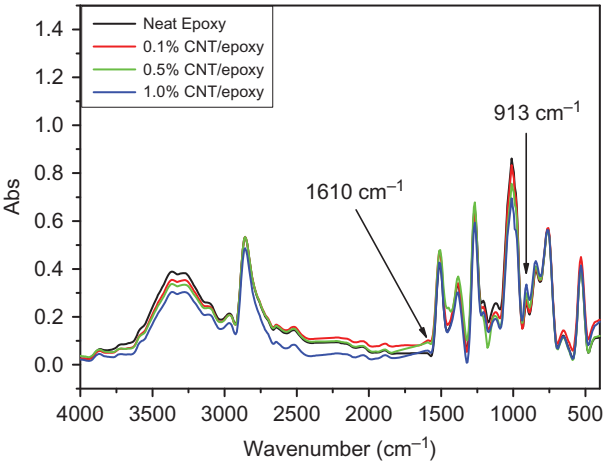

Figure 7. FTIR spectra of the cured neat epoxy and its nanocomposites.

degree of curing, which means that the band at 913 cm^{-1} can sensitively reflect the change of the epoxy groups and better obeys the Beer–Lambert law [32,36]. According to the Beer–Lambert law, the absorption peak at 1616 cm^{-1} of a benzene ring can be regarded as the internal standard, so the degree of curing can be determined from

$$\alpha = \frac{A^{1616}_{cured}A^{913}_{uncured} - A^{913}_{cured}A^{1616}_{uncured}}{A^{1616}_{cured}A^{913}_{uncured}}, \tag{3}$$

where $A_{uncured}$ is the original absorbance of neat epoxy without curing; A_{cured} is the absorbance of the cured epoxy nanocomposites. With an increase of the functionalized CNT loading, the peak area of the band at 913 cm^{-1} was increased.

The curves of the three types of CNT/epoxy nanocomposites were normalized by using the Beer–Lambert law and the peak at 913 cm^{-1} is shown in Figure 8. In terms of Equation (3), the degree of the curing of the Cl-CNT/epoxy resin nanocomposites was calculated and included in Table 2, which indicates that the curing reaction is incomplete in the Cl-CNT and Br-CNT nanocomposites. However the degree of curing of the PF_6-CNT/epoxy resin nanocomposites was about 95%. Considering the air oxidation of the curing agent, the curing of the PF_6-CNT/epoxy resin nanocomposites was close to completion. It was obvious that the degradation in the curing process of the halogen ionic liquid nanocomposites. Because part of the curing agent was oxidized before the curing,

there is little difference between the values obtained by FTIR and DSC. Different from the commercial epoxy resin, f-CNTs have functional groups as segments in polymerization. Although the mechanical and thermal loading applied on the polymer matrix can be transferred to the inserted f-CNT segments, but which are considered as defects for the curing process. In the following XPS analysis, the detailed mechanism will be discussed in the molecule level.

3.4. XPS analysis

XPS was used to characterize the surface chemical composition of the nanocomposites. It provides a quantitative evaluation of the elemental chemistry states and chemical environments. Figure 9 shows the N1*s* XPS spectra of Cl-CNT/epoxy nanocomposite. It is worth noting that the signal consists of three components corresponding to three different nitrogen species [38]. Besides the one centered at 399.8 eV, which is attributed to the protonated nitrogen atom (–NH–) coming from the amine group in the curing agent, a higher electron state was shown at 401.5 eV, which was due to quinonoid and oxidized nitrogen (–N=, N–O). There is also a signal at 403.0 eV, expected from the higher oxidization state of nitrogen in the composite [39]. This is N^+, which results from the protonation of the quinonoid imine in the ionic environment. This phenomenon is consistent with the fact that protonation occurs preferentially at the imine sites [40].

The XPS curve fitting of the C1*s* core-level spectra is shown in Figure 10. The C1*s* peak is fitted with four components centered at 284.8, 287.3, 289.2 and 291.2 eV [38]. The one of 284.8 eV results from conjugated C–C bonding of SWNTS and PANI. There was no peak that can be used to describe the C–N in this properly curve-fitted C1*s* core-level spectrum. In the 287–290 eV region, there are two peaks indicating the existence of C–O and carbonyl. The peak at 287.3 eV corresponding to C–O originates from the hydrocarbon and carbon–oxygen compounds containing oxygen with a low oxidation number component; the peak at 289.2 eV represents the carbon–oxygen and carbon–nitrogen compounds of higher oxidation number (C=O, C=N). The two oxidative states may have two possible origines; one is from curing agent, where there are some C–O groups caused from the oxidation of the curing agent by air; the other is from the CNTs and epoxy [41]. The highest one, located at 291.2 eV, is ascribed to the strong polarized C–N^+ bonding of the EpiCure W segments in the nanocomposites. The signals of the C–N component at a binding energy of 285.5 eV [38] cannot be resolved unambiguously in the C1*s* core-level spectrum when using Mg Kα excitation [42].

The above results indicate that there are two oxidation states of nitrogen in the nanocomposites, which are related to the quinonoid structure and N^+ in EpiCure W segments. This may be formed during the curing process as a consequence of both the presence of ions in the solution and the reaction of the atmospheric oxygen with amine curing agent. Therefore, it was clear that a new peak appeared in the regions of high binding energy of both C 1*s* and N 1*s* core-level spectra, respectively.

Considering that –N=, N–O and N^+ cannot react with the epoxy group, the area integrated of these two peak indicated the degree of degradation of the curing agent. For Cl-CNT/epoxy nanocomposites with 1% CNT loading, the value is 70.3%, which is very close to the degree of the curing. The curing process is proposed and schematically shown in Figure 11. Initiation is caused by the halogen radicals produced from the halogen ions and hydroxide radicals, which are the by-product from the photo-oxidation of the aniline structure. The halogen radicals were of higher activity and longer half-life at the high temperature of curing compared with room temperature.

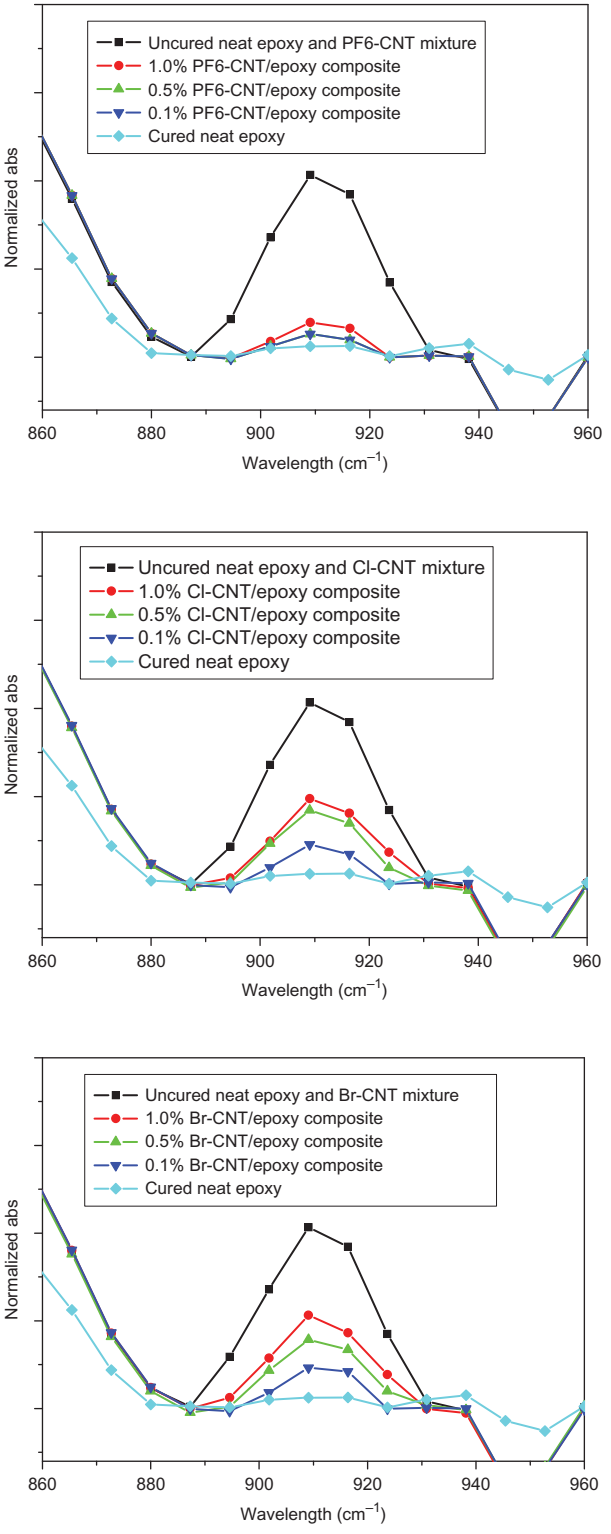

Figure 8. Normalized FTIR spectra of the cured epoxy and its nanocomposites.

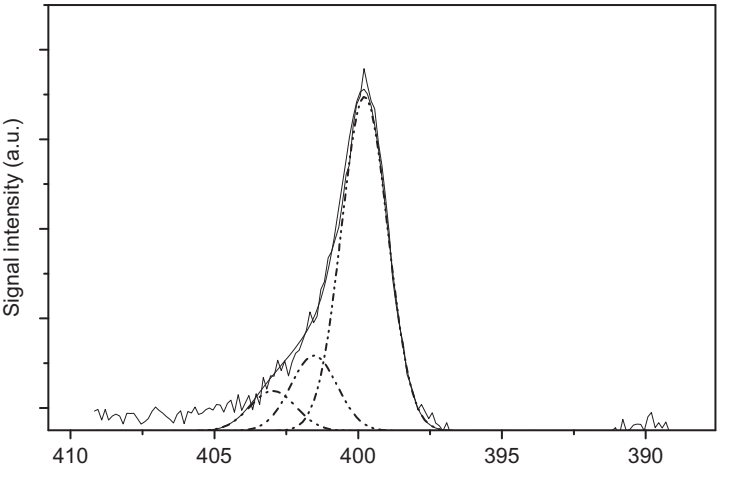

Figure 9. N1*s* core-level XPS spectra of the Cl-CNT/epoxy nanocomposites.

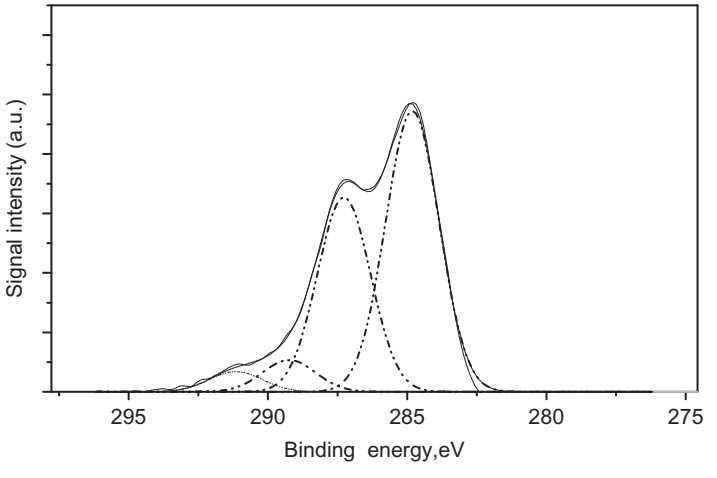

Figure 10. C1*s* core-level XPS spectra of the Cl-CNT/epoxy nanocomposites.

3.5. Mechanical and electrical properties

Four specimens were tested for each property. Stress–strain curves are shown in Figure 12 and the average mechanical properties obtained are listed in Table 3. All specimens failed immediately after the tensile stress reached its maximum value. Conceptually, the inorganic/organic nanocomposites are often expected to become stiffer and more brittle upon the incorporation of inorganic fillers [13]. For the f-CNT/epoxy nanocomposite system, the tensile strength increases with the increase of the f-CNT loading. The strong chemical bonding formed between the f-CNT and the epoxy molecules results in a good compatibility between these two phases. The improvement in the tensile strength in the case of the f-CNT/epoxy nanocomposites is attributed to the load transfer from the epoxy matrix to the tougher f-CNTs via the strong chemical bonding with only 1.00 wt% loading. Furthermore, the ions on the f-CNTs improve the dispersability of CNTs in the Epon by

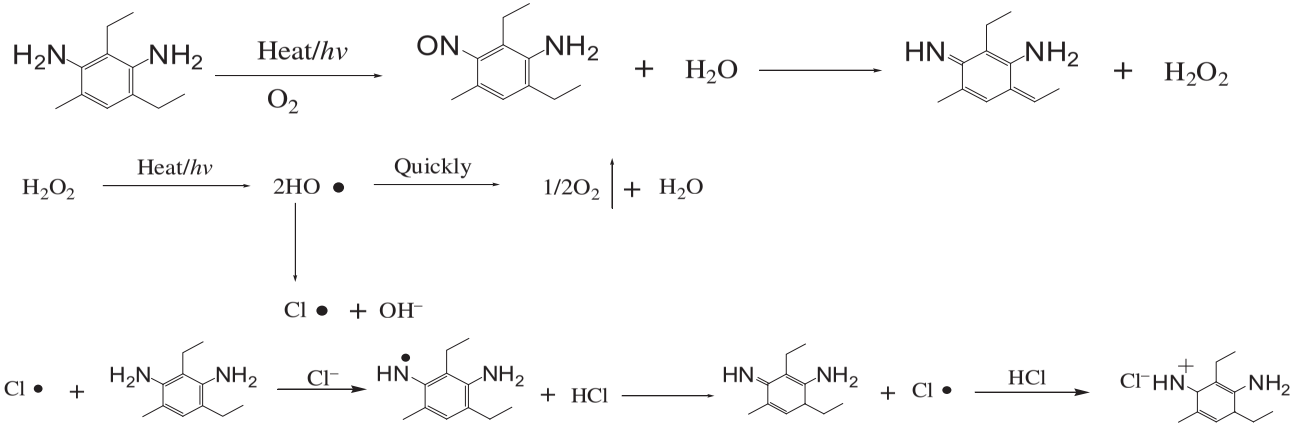

Figure 11. The assumed free radical reaction mechanism of the curing process for the Cl-CNT–epoxy nanocomposite system.

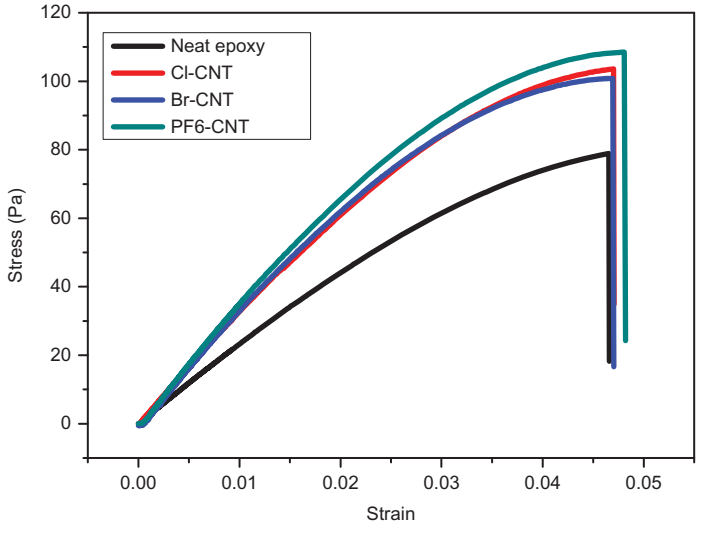

Figure 12. Stress–strain curves of tensile strength testing for neat epoxy and IL-CNT/epoxy nanocomposites.

Table 3. Tensile strength and DC conductivity of epoxy and composites with 1.0 wt% f-CNT (average values of 5 samples each).

IL-CNT loading (1.0 wt%)	Tensile strength (STDEV) (MPa)	Conductivity(STDEV) (S/cm)
Neat epoxy	78.9 ($\pm$0.2)	$<10^{-12}$
Cl-CNT	103.8 ($\pm$1.17)	3.39×10^{-3} ($\pm 0.2 \times 10^{-6}$)
Br-CNT	100.81 ($\pm$0.96)	6.06×10^{-3} ($\pm 0.1 \times 10^{-4}$)
PF_6-CNT	108.5 ($\pm$0.82)	8.38×10^{-3} ($\pm 0.5 \times 10^{-3}$)

increasing the surface polarity, which favors the dispersion of CNTs into the matrix, resulting in a larger improvement in the ultimate strength [43]. Attractively, PF_6-CNT/epoxy nanocomposites showed the largest tensile strength, as a result of the highest degree of polymerization among these three ionic liquid functionalized carbon nanotubes. The same trends were also found in the four-probe conductivity measurement. The conductivity of composites was improved dramatically as well. The conductive networks were built up by carbon nanotubes in composite matrix. From Table 3, a weaker conductive matrix was suggested in the Br-CNT nanocomposites with an uncompleted polymerization.

3.6. SEM observation of the fracture surface

Figure 13 shows SEM micrographs of the fracture surface of the same nanocomposites (0.5 and 1.0 wt%) with a thin gold sputtering for better image quality. Interestingly, the CNTs were found to be broken rather than pulled out of the surface, and most of them are embedded in and tightly held to the matrix, indicating a strong interfacial bonding between the epoxy matrix and the functionalized CNTs, which is responsible for the enhanced mechanical properties.

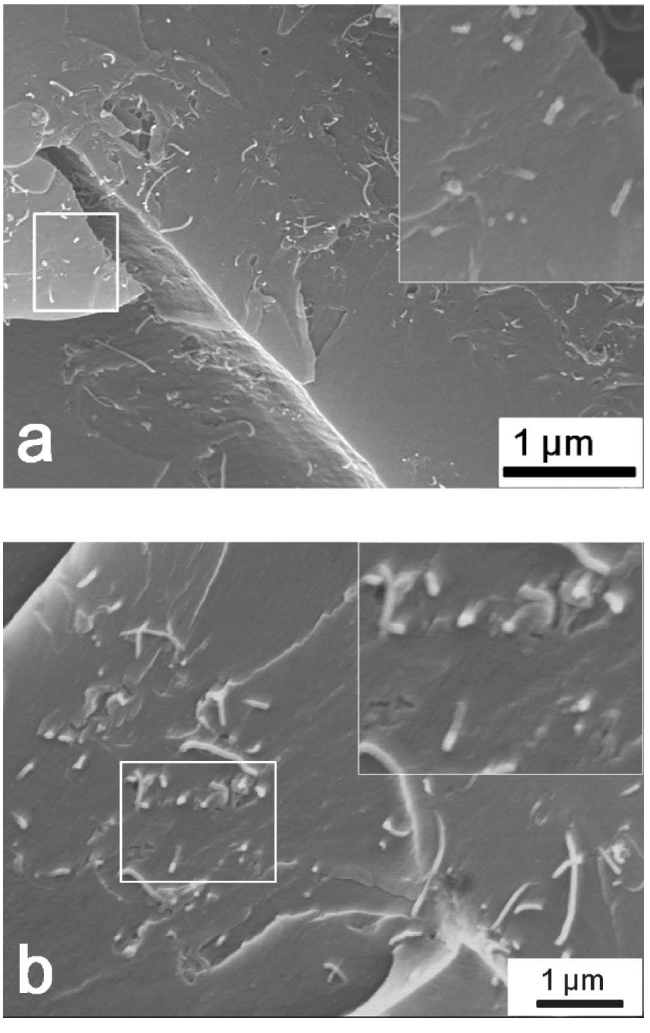

Figure 13. SEM image of the fracture surface of the nanocomposites having an IL-CNT concentration of 0.5 wt% (a) and 1.0 % (b), using an acceleration voltage of 5 kV.

4. Conclusion

In this work, the effects of the anion from ionic liquids on the curing behavior of an epoxy resin were investigated using differential scanning calorimetry (DSC) and Fourier transform infrared (FTIR) spectroscopy. The PF_6-CNT/epoxy nanocomposites and neat epoxy have the same curing process, whereas Cl-CNT and Br-CNT/epoxy nanocomposites were affected by the halogen anions in the curing. Two different reaction mechanisms are proposed for the curing process. As the curing proceeds, the enthalpy of reaction decreases in the epoxy nanocomposites, with the largest decrease observed in the Br-CNT/epoxy system. As curing progresses, the values of heat for the neat resin and PF_6-CNT epoxy nanocomposite samples are relatively the same, whereas they are significantly lower for the Cl-CNT and Br-CNT nanocomposite samples. Comparison of the degree of curing and concentration of products suggests that the cure mechanisms of the neat resin and PF_6-CNT/epoxy composite are similar but different from the Cl-CNT and Br-CNT samples. IL-CNTs demonstrate a remarkable enhancement of the DC

conductivity at low-weight loadings and tensile strength significantly outperforms other carbon nanotube-based fillers as a result of the strong chemical bonding, as indicated from the SEM microstructures of the fracture surface.

Acknowledgments

This paper is based on work supported by the NBIT Program funded jointly by the Ministry of Science and Technology of Korea and the US Air Force Office of Scientific Research. Dr. Z. Guo appreciates the support from the National Science Foundation - Nanoscale Interdisciplinary Research Team (NIRT) and Materials Processing and Manufacturing (CMMI 10-30755). Thanks for NSF IGERT: Materials Creation Training Program (MCTP) -DGE-0654431 and the California Nano Systems Institute.

References

[1] H.D. Wagner, O. Lourie, Y. Feldman, and R. Tenne, *Stress-induced fragmentation of multiwall carbon nanotubes in a polymer matrix*, Appl. Phys. Lett. 72 (1998), pp. 188–190.
[2] P.M. Ajayan, L.S. Schadler, C. Giannaris, and A. Rubio, *Single-walled carbon nanotube–polymer composites: strength and weakness*, Adv. Mater. 12 (2000), pp. 750–753.
[3] A.B. Dalton, S. Collins, E. Muñoz, J.M. Razal, V.H. Ebron, J.P. Ferraris, J.N. Coleman, B.G. Kim, and R.H. Baughman, *Super-tough carbon nanotube fibres*, Nature 423 (2003), pp. 703–703.
[4] M. Terrones, *Science and technology of the twenty-first century: synthesis, properties, and applications of carbon nanotubes*, Annu. Rev. Mater. Res. 33 (2003), pp. 419–501.
[5] P. Gajendran and R. Saraswathi, *Polyaniline–carbon nanotube composites*, Pure Appl. Chem. 80 (2008), pp. 2377–2395.
[6] E.J. Garcia, A.J. Hart, B.L. Wardle, and A. Slocum, *Fabrication and nanocompression testing of aligned CNT/polymer nanocomposites*, Adv. Mater. 19 (2007), pp. 2151–2156.
[7] P.M. Ajayan and J.M. Tour, *Nanotube composites*, Nature 447 (2007), pp. 1066–1068.
[8] S.M. Yuen, C.C.M. Ma, C.L. Chiang, Y.Y. Lin, and C.C. Teng, *Preparation and morphological, electrical, and mechanical properties of polyimide-grafted MWCNT/polyimide composite*, J. Polymer Sci. A Polymer Chem. 45 (2007), pp. 3349–3358.
[9] J.R. Capadona, O. Van Den Berg, L.A. Capadona, M. Schroeter, S.J. Rowan, D.J. Tyler, and C. Weder, *Self-Assembled nanofiber templates: a versatile approach for the processing of polymer nanocomposites*, Nat. Nanotech. 2 (2007), pp. 765–769.
[10] Z. Wang, M. Lu, H.L. Li, and X.Y. Guo, *SWNTs–polystyrene composites preparations and electrical properties research*, Mater. Chem. Phys. 100 (2006), pp. 77–81.
[11] N. Li, Y. Huang, F. Du, X.B. He, X. Lin, H.J. Gao, Y.F. Ma, F.F. Li, Y.S. Chen, and P.C. Eklund, *Electromagnetic interference (EMI) shielding of single-walled carbon nanotube epoxy composites*, Nano Lett. 6 (2006), pp. 1141–1145.
[12] J. Sandler, M.S.P. Shaffer, T. Prasse, W. Bauhofer, K. Schulte, and A.H. Windle, *Development of a dispersion process for carbon nanotubes in an epoxy matrix and the resulting electrical properties*, Polymer 40 (1999), pp. 5967–5971.
[13] C.H. Tseng, C.C. Wang, and C.Y. Chen, *Functionalizing carbon nanotubes by plasma modification for the preparation of covalent-integrated epoxy composites*, Chem. Mater. 19 (2007), pp. 308–315.
[14] L. Sun, G.L. Warren, J.Y. O'Reilly, W.N. Everett, S.M. Lee, D. Davis, D. Lagoudas, and H.J. Sue, *Mechanical properties of surface-functionalized epoxy/SWCNT nanocomposites*, Carbon 46 (2008), pp. 320–328.
[15] J. Zhu, J.D. Kim, H.Q. Peng, J.L. Margrave, V.N. Khabashesku, and E.V. Barrera, *Improving the dispersion and integration of single-walled carbon nanotubes in epoxy composites through functionalization*, Nano Lett. 3 (2003), pp. 1107–1113.
[16] X.Y. Gong, J. Liu, S. Baskaran, R.D. Voise, and J.S. Young, *Surfactant-assisted processing of carbon nanotube/polymer composites*, Chem. Mater. 12 (2000), pp. 1049–1052.
[17] J. Li, P.C. Ma, W.S. Chow, C.K. To, B.Z. Tang, and J.K. Kim, *Correlations between percolation threshold, dispersion state, and aspect ratio of carbon nanotubes*, Adv. Funct. Mater. 17 (2007), pp. 3207–3215.
[18] J. Zhu, H. Peng, F. Rodriguez-Macias, J. Margrave, V. Khabashesku, A. Imam, K. Lozano, and E. Barrera, *Reinforcing of epoxy polymer composites through integration of functionalized nanotubes*, Adv. Funct. Mater. 14 (2004), pp. 643–648.

[19] T. Welton, *Room-temperature ionic liquids. Solvents for synthesis and catalysis*, Chem. Rev. 99 (1999), pp. 2071–2083.
[20] R.D. Rogers and K.R. Seddon, *Ionic Liquids as Green Solvents: Progress and Prospects*, American Chemical Society, Washington DC, 2003.
[21] H. Ohno, *Electrochemical Aspects of Ionic Liquids*, John Wiley & Sons, New Jersey, 2005.
[22] P. Wasserscheid and T. Welton, *Ionic Liquids in Synthesis*, Wiley-VCH, Weinheim, 2003.
[23] J. Zhu, S. Wei, R. Patil, D. Rutman, A.S. Kucknoor, A. Wang, and Z. Guo, *Ionic liquid assisted electrospinning of quantum dots/elastomer nanocomposite fibers*, Polymer 52 (2011), pp. 1954–1962.
[24] H. Ohno, M. Yoshizawa, and W. Ogihara, *A new type of polymer gel electrolyte: zwitterionic liquid/polar polymer mixture*, Electrochim. Acta 48 (2003), pp. 2079–2083.
[25] E. Andrzejewska and I. Stepniak, *Highly conductive solid polymer-(ionic liquid) electrolytes prepared by* in situ *photopolymerization*, Polimery 51 (2006), pp. 859–861.
[26] A. Noda and M. Watanabe, *Highly conductive polymer electrolytes prepared by* in situ *polymerization of vinyl monomers in room temperature molten salts*, Electrochim. Acta 45 (2000), pp. 1265–1270.
[27] S. Washiro, M. Yoshizawa, H. Nakajima, and H. Ohno, *Highly ion conductive flexible films composed of network polymers based on polymerizable ionic liquids*, Polymer 45 (2004), pp. 1577–1582.
[28] H. Ohno, M. Yoshizawa, and W. Ogihara, *Development of new class of ion conductive polymers based on ionic liquids*, Electrochim. Acta 50 (2004), pp. 255–261.
[29] M.J. Park and S.G. Lee, *Palladium catalysts cupported onto the ionic liquid-functionalized carbon nanotubes for carbon–carbon coupling*, Bull. Kor. Chem. Soc. 28 (2007), pp. 1925–1926.
[30] M.J. Park, J.K. Lee, B.S. Lee, Y.W. Lee, I.S. Choi, and S.G. Lee, *Covalent modification of multiwalled carbon nanotubes with imidazolium-based ionic liquids: effect of anions on solubility*, Chem. Mater. 18 (2006), pp. 1546–1551.
[31] M. Abdalla, D. Dean, P. Robinson, and E. Nyairo, *Cure behavior of epoxy/MWCNT nanocomposites: the effect of nanotube surface modification*, Polymer 49 (2008), pp. 3310–3317.
[32] S. Jana and W.H. Zhong, *FTIR study of ageing epoxy resin reinforced by reactive graphitic nanofibers*, J. Appl. Polymer Sci. 106 (2007), pp. 3555–3563.
[33] K.T. Lau, M. Lu, C.K. Lam, H.Y. Cheung, F.L. Sheng, and H.L. Li, *Thermal and mechanical properties of single-walled carbon nanotube bundle-reinforced epoxy nanocomposites: the role of solvent for nanotube dispersion*, Compos. Sci. Tech. 65 (2005), pp. 719–725.
[34] K. Yang, M.Y. Gu, and Y.P. Jin, *Cure behavior and thermal stability analysis of multiwalled carbon nanotube/epoxy resin nanocomposites*, J. Appl. Polymer Sci. 110 (2008), pp. 2980–2988.
[35] L. Valentini, D. Puglia, F. Carniato, E. Boccaleri, L. Marchese, and J.M. Kenny, *Use of plasma fluorinated single-walled carbon nanotubes for the preparation of nanocomposites with epoxy matrix*, Compos. Sci. Tech. 68 (2008), pp. 1008–1014.
[36] F. Fraga, E.C. Vazquez, E. Rodriguez-Nunez, and J.M. Martinez-Ageitos, *Curing kinetics of the epoxy system diglycidyl ether of bisphenol a/isophoronediamine by fourier transform infrared spectroscopy*, Polymer Adv. Tech. 19 (2008), pp. 1623–1628.
[37] D.Y. Shen, *The Application of the Fourier Transform Infrared Spectroscopy in Polymer Study*, Academic Press, Beijing, 1982.
[38] G. Muilenberg, *Handbook of X-ray Photoelectron Spectroscopy*, Perkin Elmer New York, 1997.
[39] J.F. Shen, W.S. Huang, L.P. Wu, Y.Z. Hu, and M.X. Ye, *Thermo-physical properties of epoxy nanocomposites reinforced with amino-functionalized multi-walled carbon nanotubes*, Compos. Appl. Sci. Manuf. 38 (2007), pp. 1331–1336.
[40] A.G. MacDiarmid, J.C. Chiang, A.F. Richter, and A. Epstein, *Polyaniline: a new concept in conducting polymers*, Synth. Met. 18 (1987), pp. 285–290.
[41] E.T. Kang, K.G. Neoh, and K. Tan, *Polyaniline: a polymer with many interesting intrinsic redox states*, Progr. Polymer Sci. 23 (1998), pp. 277–324.
[42] Y. Chen, E.T. Kang, K.G. Neoh, S.L. Lim, Z.H. Ma, and K.L. Tan, *Intrinsic redox states of polyaniline studied by high-resolution X-ray photoelectron spectroscopy*, Colloid Polymer Sci. 279 (2001), pp. 73–76.
[43] F.H. Gojny, M.H.G. Wichmann, B. Fiedler, and K. Schulte, *Influence of different carbon nanotubes on the mechanical properties of epoxy matrix composites – a comparative study*, Compos. Sci. Tech. 65 (2005), pp. 2300–2313.